JOURNAL OF CHEMICAL & ENGINEERING DATA

ARTICLE

pubs.acs.org/jced

Phase Separation and Interfacial Viscoelasticity of Charge-Neutralized Heavy Oil Nanoemulsions in Water

Chandra W. Angle* and Yujuan Hua

CanmetENERGY, Natural Resources Canada, Devon, Alberta, Canada T9G 1A8

ABSTRACT: Steam-assisted gravity drainage processes for heavy oil recovery produce extremely stable nanoemulsions that remain dispersed in water for years if left untreated. The need to produce clean water for recycling demands that the nanoemulsions be destabilized and the oil phase separated from the water. The destabilization of these nanoemulsions requires an understanding of the nature of the oil−water interface. In this paper, the ζ potential and sizes of the nanoemulsions were measured with and without treatment with a cationic polymer. The coalescence of nanoemulsions was monitored by size changes using dynamic light scattering, microscopy, and water-phase separation kinetics. Small-deformation pendant drop oscillation was used to measure the dilational viscoelasticity of the oil−water interface with and without polymer adsorption. The results indicated that both the size and the large negative ζ potential contribute to the stability of the nanoemulsions in water. The addition of polymer not only causes charge neutralization but also enhances the interfacial activity and modifies the interfacial dilational viscoelasticity. The viscoelasticity is dependent on the frequency of droplet oscillation. Polymer adsorption modifies these interfacial properties while enabling coalescence and phase separation.

INTRODUCTION

In situ emulsions of heavy oil in water that are produced in steam-assisted gravity drainage (SAGD) production facilities must be destabilized for water-phase separation and recovery of the oil. Cleaning the produced water reduces the cost and the harm to the environment. In the past, much effort has been devoted to understanding properties of heavy oils,[1−3] the stability of heavy[1,4−8]and light crude oil emulsions,[9−16] and heavy-oil emulsion destabilization and its mechanisms.[17,18] However, in spite of this body of work, there are still challenges in treating and understanding nanosized emulsions. New tools such as oscillating longitudinal waves, oscillating drop, and capillary pressure methods are now available for studying interfaces, providing the opportunity to gain in-depth insight into the mechanisms while destabilizing the interfaces. Studies of the interfacial dilational rheology of light crude, bituminous, and heavy oil/water systems with and without adsorbed surfactants are still limited,[9,11,12,14,16,17,19−37] and the use of these techniques to study the destabilization of heavy-oil systems is still sparse.[9,25,26,31,38−40] There is also a limited understanding of very low American Petroleum Institute (API) gravity heavy-oil interfaces during charge neutralization by cationic polymer interactions [where the API gravity is given in units of °API by the expression 141.5/(specific gravity) − 131.5, referenced at 288.75 K and atmospheric pressure]. The effects of the frequency of oscillation on the heavy-oil interfacial viscoelastic properties under these conditions need attention. This paper addresses this gap.

This work investigated the destabilization of a very low API gravity heavy oil that forms extremely stable nanoemulsions after SAGD extractions. We characterized the oil and the emulsions by measurements of size and ζ potential before and after charge neutralization using a cationic polymer. We followed the destabilization by water-resolution kinetics, microscopic images of the coalescing drops, and sizes of aggregates. We characterized the interfaces first by measuring the dynamic interfacial tension (σ_{dyn}) and second by determining the equilibrium interfacial tension (σ^{eq}). The σ^{eq} values were used to determine the oil concentration at monolayer coverage of the oil−water interface and the Gibbs surface excess. Interfacial dilational rheology was measured using pendant-drop oscillation as a function of the frequency of oscillation, residence time in the continuous phase, and cationic polymer concentration.

EXPERIMENTAL SECTION

Materials and Methods. Heavy-oil emulsions were obtained from a SAGD deep-well extraction operation from Northern Alberta, Canada. The API gravity of the heavy oil was 7.5 °API. SARA (saturates, aromatics, resins, and asphaltenes) analysis of the oil gave mass fractions of 0.117, 0.320, 0.416, and 0.147 for saturates, aromatics, resins or polars, and asphaltenes, respectively. The number-average molecular weight of the heavy oil was measured to be 546.4 $g \cdot mol^{-1}$ using vapor-pressure osmometry (K-7000 KNAUER, Berlin, Germany) in toluene at 50 °C. The in situ emulsions were characterized for sizes and ζ potentials with a Zeta-Nanosizer instrument (Malvern Instruments, Westborough, MA) upon dilution in a buffer containing 0.01 $mol \cdot kg^{-1}$ sodium bicarbonate ($NaHCO_3$, ACS grade, Fisher Scientific) prepared in high-purity Millipore deionized water (resistivity 18 MΩ, surface tension 72.9 $mN \cdot m^{-1}$). The polymer used for destabilization was a high-purity cationic polyethyleneimine, $(C_2H_5N)_n$, having a molecular weight of 40 000 $g \cdot mol^{-1}$

Special Issue: John M. Prausnitz Festschrift

Received: October 30, 2010
Accepted: January 11, 2011
Published: February 08, 2011

(Polysciences, Inc., Warrington, PA). It was dissolved in the 0.01 mol·kg^{-1} $NaHCO_3$ buffer to make a $5\cdot10^{-5}$ mol·kg^{-1} stock polymer solution prior to its addition to the emulsions for demulsification or to the cuvette containing 0.01 mol·kg^{-1} $NaHCO_3$ for dilational viscoelastic studies. The pH values of all aqueous liquids were measured using a Fisher Research AR-50 meter and combination glass electrodes (model 300729, Denver Instruments, Bohemia, NY) standardized with pH 4, pH 8, and pH 10 buffers (Fisher Scientific).

The emulsion stability was followed at 296.15 K by measurement of the ζ potential and size of droplets after the polymer was added at lower dosages of (0, 2.5, 6.25, 10, 12.5, and 25)·10^{-9} mol·kg^{-1}. The field in situ emulsions were diluted to a volume fraction of 0.0025 in the $NaHCO_3$ buffer, whose ionic strength was similar to that of the in situ water.

Duplicate 10 mL aliquots of in situ emulsion were also placed in centrifuge tubes, and $1\cdot10^{-6}$ mol·kg^{-1} polymer was added to account for a more concentrated nanoemulsion population. The tubes were capped, hand-mixed by 10 end-to-end inversions, and allowed to stand undisturbed at 296.15 K. After fixed incubation times, volumes of resolved water were measured and plotted as a function of incubation time. At the same times, microscopic images of the destabilized oil/water emulsions on 10 μm depth quartz slides (Helma, Canada) were recorded with a Nikon Eclipse E600 microscope equipped with a Nikon Coolpix AE950 digital camera and Plan Fluor ELWD 40× DICM objective and transmitted light microscopy.

Before the interfacial tension experiments were performed, the heavy oil was placed into glass jars containing preweighed amounts of toluene (optima grade, Fisher Scientific), after which the jars were sealed. The oil was dissolved by wrist-action shaking for 2 h until no lumps were seen by microscopy. Heavy-oil-in-toluene concentrations of (0.000183, 0.00183, 0.00915, 0.0183, 0.0458, 0.0915, 0.183, 0.274, and 0.458) mol·kg^{-1} were prepared for interfacial analysis by the axisymmetric drop profile method. The dynamic interfacial tension at each concentration of diluted heavy oil was measured as a function of drop aging time in the 0.01 mol·kg^{-1} $NaHCO_3$ buffer. In this technique, a 20 μL drop (interfacial area A = 34.5 mm^2) was expelled from a 250 μL syringe to the tip of a U-shaped needle immersed in the aqueous phase (Tracker, Teclis-ITConcept, France). Dynamic interfacial tensions $\sigma_{i(t)}$ of the fresh oil droplet in the $NaHCO_3$ buffer were measured until near-equilibrium was achieved at 296.15 K. To obtain σ^{eq}, methods described previously[5,6] were used to fit the data to a Gibbs diffusion-limited kinetic model (eq 1):

$$\sigma_{i(t)} = \sigma_0 \exp\left[-(\beta t)^{1/2}\right] + \sigma^{eq} \quad (1)$$

where $\sigma_{i(t)}$ is interfacial tension at time t, σ_0 is a parameter calculated as the difference between $\sigma_{i(t)}$ and the equilibrium interfacial tension σ^{eq} at t = 0, and β is a kinetic parameter related to a diffusion constant representing the adsorption rate. Numerical methods were used to fit eq 1 to the experimental data and in the determination of the parameters and coefficients.

A plot of σ^{eq} versus ln c_s, where c_s is the concentration of heavy oil, was fitted to the Gibbs adsorption model,

$$\Gamma = -\frac{1}{RT}\frac{\partial\sigma^{eq}}{\partial(\ln c_s)} \quad (2)$$

in order to obtain Γ, the surface excess concentration of surface-active agent adsorbed at the interface. In eq 2, the quantity $[\partial\sigma^{eq}/\partial(\ln c_s)]$ represents the slope of a straight-line plot of σ^{eq} versus ln c_s, R is the universal gas constant (8.314 J·K^{-1}·mol^{-1}), and T is the thermodynamic absolute temperature.

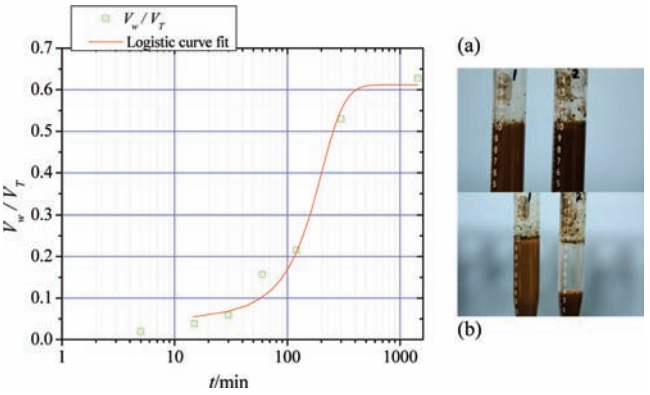

Figure 1. Fraction of resolved water as a function of time t for oil/water emulsions (a) before (top photograph) and (b) 24 h after (bottom photograph) addition of $1\cdot10^{-6}$ mol·kg^{-1} polymer. V_W is the volume of resolved water and V_T the total volume. The line is a logistic fit to guide the eye.

Principles of Interfacial Dilational Rheology. Small harmonic dilational oscillation of a heavy oil drop should result in periodic expansion and compression of the adsorbed layer of surface-active components covering the interface.[41−45] The consequence is a dilational stress expressed as the change in interfacial tension periodically. This dilational stress is revealed as a periodic change in interfacial tension, Δγ, with the same frequency of oscillation:

$$\Delta\gamma = \gamma(t) - \gamma_0 \quad (3)$$

where γ_0 is the initial interfacial tension and $\gamma(t)$ is the interfacial tension in the period or time t. Thus, if the dilational response is completely elastic, the interfacial stress is directly proportional to the area variation, α, which is defined by the expression $\alpha = \Delta A/A_0 = [A(t) - A_0]/A_0$, in which $A(t)$ is the interfacial area at time t and A_0 is the reference interfacial area. However, the dilational stress is the sum of a purely elastic term and a purely viscous term. The viscous term is the rate of change of the area variation (or rate of interface deformation), $\dot{\alpha}$. For adsorbed layers that exhibit relaxation, the system is described as viscoelastic, and relaxation occurs at the interface as well as in the bulk. The complex viscoelastic modulus E thus describes the relationship between dilational stress and area. E is also called the complex dilational viscoelastic modulus or the dilational viscoelasticity. The dilational stress is

$$\Delta\gamma = E_0\alpha + \eta\dot{\alpha} \quad (4)$$

where the coefficient E_0 is the dilational interfacial elasticity and η is the dilational interfacial viscosity. Thus, a small-amplitude periodic perturbation at frequency ν also results in an area perturbation, which can be expressed as

$$\Delta A = \tilde{A}e^{i2\pi\nu t} \quad (5)$$

in which ΔA is the change in interfacial area, $\tilde{A}$ is the amplitude of the area oscillation, and ν is the sinusoidal oscillation frequency. The change in the interfacial area is also termed the interfacial deformation. The dilational

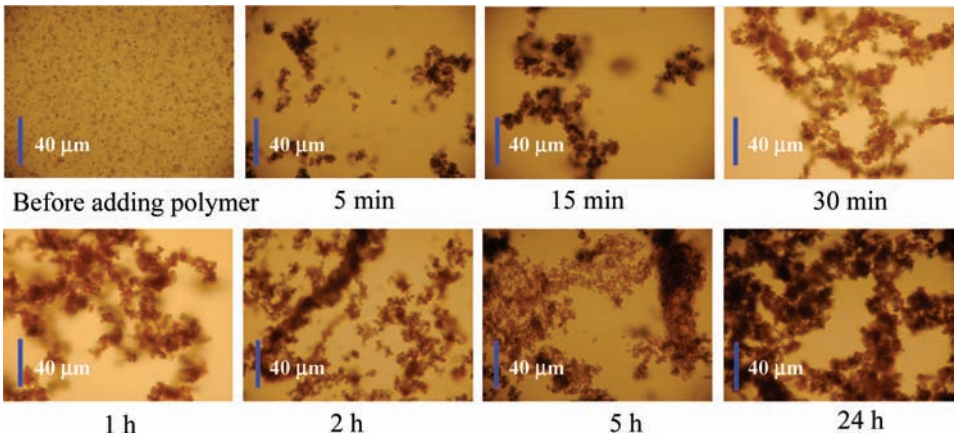

Figure 2. Micrographs of oil droplets in water before addition and as a function of time t after addition of $1 \cdot 10^{-6}$ mol·kg^{-1} polymer. Scale bars = 40 μm.

Table 1. Average ζ Potential and Sizes of Emulsions and Aggregates in 0.01 mol·kg^{-1} $NaHCO_3$ before and Immediately after Polymer Addition

concentration of polymer c_p mol·kg^{-1}	ζ potential/ mV	z-avg drop size /nm	repeat z-avg size/nm (aged emulsions)
0	−98.5 ± 3.8	776.3 ± 38.1	
$2.5 \cdot 10^{-9}$	−78.8 ± 4.0	1229 ± 228	
$6.25 \cdot 10^{-9}$	−24.8 ± 2.2	1735 ± 248	1298 ± 140
$10 \cdot 10^{-9}$	−6.4 ± 1.1	1335 ± 148	1713 ± 181
$12.5 \cdot 10^{-9}$	5.4 ± 3.9, −4.6 ± 6.6, 0.2 ± 3.8	1487 ± 36	1530 ± 80
$25 \cdot 10^{-9}$	10.8 ± 2.4	1511 ± 296	

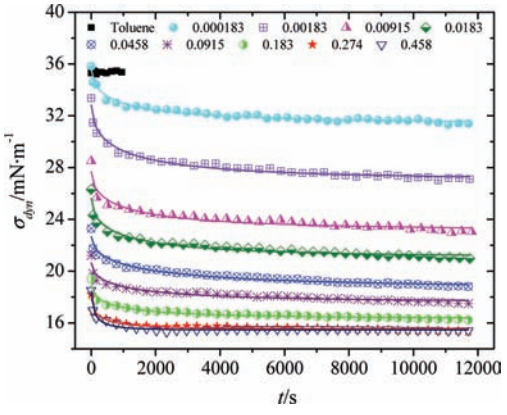

Figure 3. Dynamic interfacial tensions σ_{dyn} for various concentrations of heavy oil in toluene/0.01 mol·kg^{-1} $NaHCO_3$ as functions of time. Lines are fits to eq 1.

viscoelasticity E is thus the complex number whose real part is the dilational elasticity E_0 and whose imaginary part is $E_i = 2\pi\nu\eta$, which is called the dilational viscous modulus:

$$E = \frac{\Delta\gamma}{\alpha} = E_0 + i2\pi\nu\eta = E_0 + iE_i \qquad (6)$$

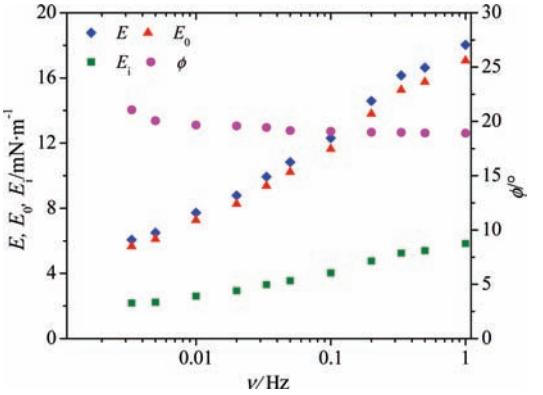

Figure 4. Effect of oscillation frequency ν on the viscoelastic modulus E, elastic modulus E_0, viscous modulus E_i, and phase angle ϕ of 0.183 mol·kg^{-1} heavy oil in toluene/0.01 mol·kg^{-1} $NaHCO_3$. The interface was aged for 15 h.

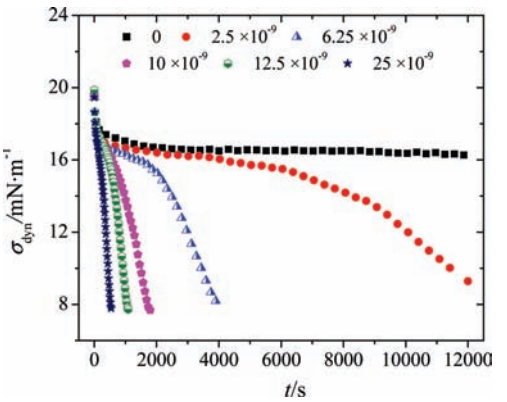

Figure 5. Dynamic interfacial tension σ_{dyn} for the 0.183 mol·kg^{-1} heavy-oil-in-toluene−$NaHCO_3$ interface at increased polymer dosages (mol·kg^{-1}) added to the water phase.

For a low-amplitude perturbation, $E(\nu)$ or E can be simply expressed using the linear Fourier formalism:[44−46]

$$\Delta\gamma = \int_0^t \bar{E}(\tau)\alpha(t - \tau)\, d\tau \qquad (7)$$

dx.doi.org/10.1021/je101162n |J. Chem. Eng. Data 2011, 56, 1388–1396

Table 2. Values of σ^{eq} for Increasing Concentrations of the Heavy Oil in Toluene/$NaHCO_3$ System

$c_s/(10^{-3}\cdot$ mol·kg$^{-1})$	0.183	1.83	9.15	18.3	45.8	91.5	183	274	458
σ^{eq}/mN·m^{-1}	31.31	26.86	22.43	20.77	18.24	17.01	16.13	15.49	15.46
R^2	0.935	0.964	0.948	0.965	0.981	0.951	0.963	0.936	0.976

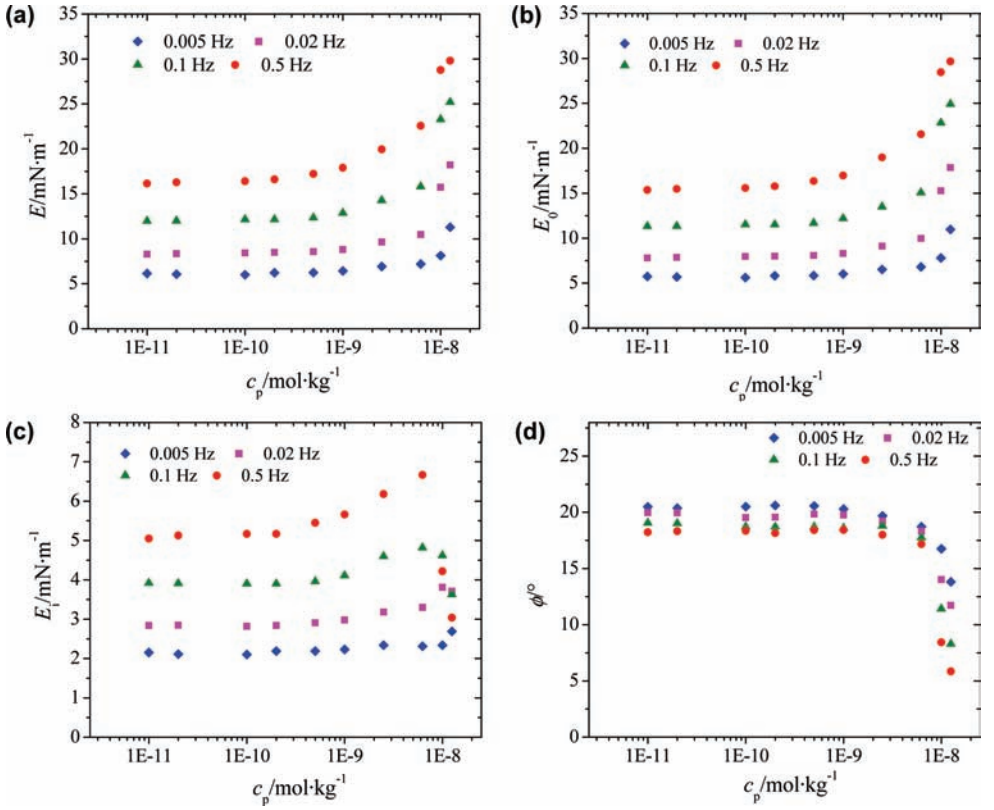

Figure 6. Dependence of (a) viscoelastic modulus (E), (b) elastic modulus (E_0), (c) viscous modulus (E_i), and (d) phase angle (ϕ) on polymer concentration (c_p) at various frequencies of oscillation for a 0.183 mol·kg^{-1} heavy-oil-in-toluene−$NaHCO_3$ interface.

where τ is the relaxation time. The frequency-dependent complex modulus $E(\nu)$ can also be envisaged as the transfer function of the interfacial layer, and is the inverse Fourier transform of $E(\nu)$. In the oscillating drop experiments at a given frequency, the area is defined as

$$A = A_0 + \tilde{A}\sin(2\pi\nu t) \tag{8}$$

and the harmonic response of the interfacial tension is

$$\gamma = \gamma_0 + \tilde{\gamma}\sin(2\pi\nu t + \phi) \tag{9}$$

where $\tilde{\gamma}$ is the amplitude of the interfacial tension oscillation, and ϕ is the phase shift between the area oscillation and the interfacial tension response, which is equal to the phase shift for the complex dilational modulus E in the expression

$$E = \frac{\tilde{\gamma}}{\tilde{A}/A_0}\exp(i\phi) \tag{10}$$

In our work, low-deformation dilational viscoelastic measurements were conducted for conditions just below the critical aggregation concentration (CAC) of the heavy-oil-in-toluene surfactants adsorbed at the oil/water interface. In this technique, the control drop was left to equilibrate in the aqueous phase overnight (15 h). Harmonic oscillation of the area of the aged drop allowed periodic expansion and compression of the adsorbed interfacial layer. The sinusoidal oscillation was done for a range of frequencies [(0.0033 to 1.0) Hz]. A small-amplitude controlled sinusoidal oscillation of 10 % of the area or approximately 3.45 mm^2 was used to maintain the linearity of the response according to eq 6. This initiated relaxation processes that resulted in periodic variations in the interfacial tension at the same frequency. The small-amplitude controlled harmonic perturbation permitted the magnitude and phase of the interfacial tension response to be harmonic, in direct correlation with eq 6.

Following the equilibration of the drop, the polymer was added to the water phase and mixed in for 1 min, after which the dilational rheological measurements were conducted. Frequency sweeps were repeated every 15 min by controlled oscillation at increasing frequencies of (0.005, 0.02, 0.1, and 0.5) Hz and decreasing periods of (200, 50, 10, and 2) s, respectively. Each sequence took 12 min of frequency scanning and 3 min of rest. The sequence was repeated until the drop detached. As soon as drop detachment occurred, the experiments were stopped for the polymer-adsorbed systems. Images of the drops were captured by a CCD camera and used to determine the interfacial tension and area variation during the oscillation. These drop oscillation techniques are described in detail elsewhere.[47]

dx.doi.org/10.1021/je101162n |J. Chem. Eng. Data 2011, 56, 1388–1396

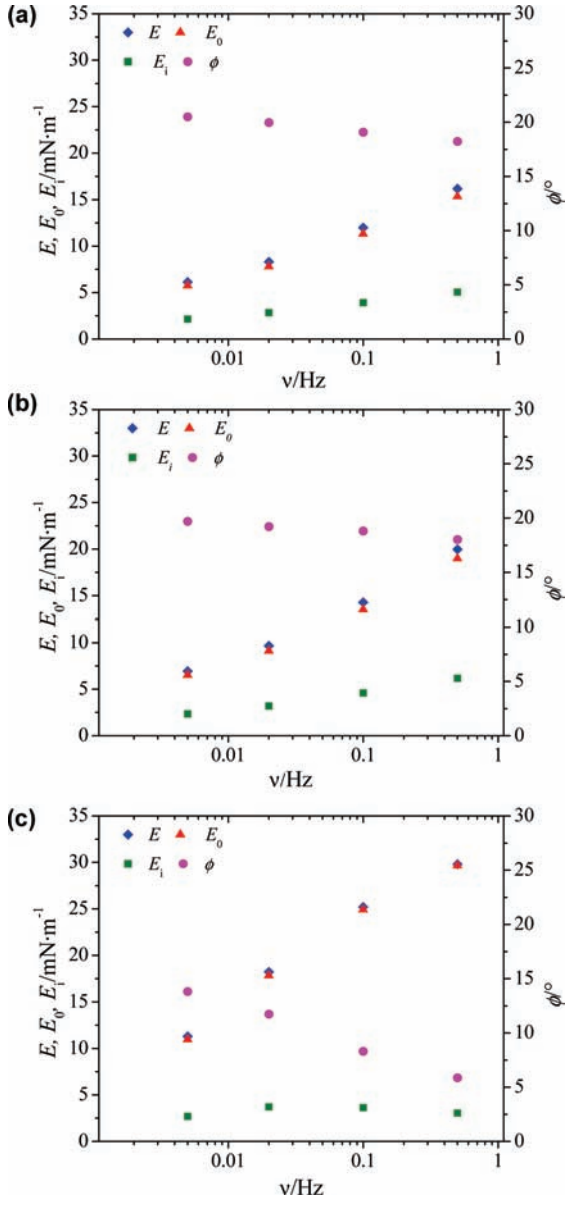

Figure 7. Comparisons of E, E_0, E_i, and ϕ as functions of frequency (ν) for polymer concentrations of (a) $1 \cdot 10^{-11}$ mol·kg^{-1}, (b) $2.5 \cdot 10^{-9}$ mol·kg^{-1}, and (c) $12.5 \cdot 10^{-9}$ mol·kg^{-1} in the water phase of a 0.183 mol·kg^{-1} heavy-oil-in-toluene−$NaHCO_3$ interface.

RESULTS AND DISCUSSION

Figure 1 shows the resolved water-phase separation kinetics from the fine nanoemulsions destabilized by addition of $1 \cdot 10^{-6}$ mol·kg^{-1} polymer. Photographs of the water and oil phases (a) before and (b) after phase separation are shown at the right. Figure 2 shows microscope images of the in situ emulsion droplets before polymer addition and as they aggregated and coalesced over the 24 h period after polymer addition. Figure 2 also shows the sequential growth of oil droplet sizes in time by coalescence. The formation of aggregates through flocculation of the nanoemulsions is also shown. As the clusters became larger, they were prone to settling because the density of the heavy oil was greater than that of water. Aggregation was caused by electrostatic attraction of oppositely charged droplets, which were partially covered with polymer that neutralized the droplets' negative charges (Table 1).

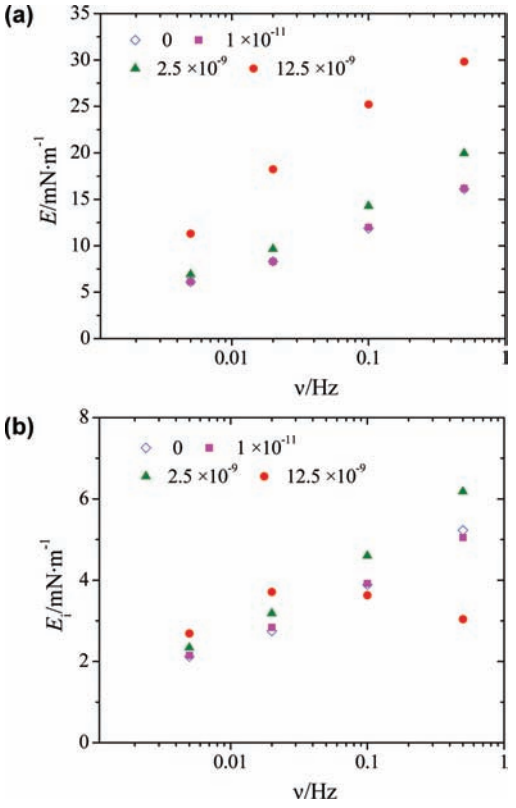

Figure 8. Comparisons of (a) E and (b) E_i as functions of frequency (ν) for polymer concentrations of (0 to 12.5)$\cdot 10^{-9}$ mol·kg^{-1} in the aqueous phase of a 0.183 mol·kg^{-1} heavy-oil-in-toluene−$NaHCO_3$ interface.

Drop−drop attraction thus facilitated coalescence by drop−drop contact and film drainage. The ζ potential and size data appear in Table 1. The data show that charge neutralization as a result of polymer addition for a dilute emulsion system was accompanied by a growth in the z-average size until complete neutralization occurred at $12.5 \cdot 10^{-9}$ mol·kg^{-1} polymer. The repeat measurements at $12.5 \cdot 10^{-9}$ mol·kg^{-1} showed a teetering above and below zero ζ potential. Here the aggregate sizes were maximized at 1530 nm. The average droplet/aggregate size remained approximately the same after charge reversal at $25 \cdot 10^{-9}$ mol·kg^{-1}polymer. It was expected that there would be further aggregate and drop growth with time, as shown in the micrographs of Figure 2.

Interfacial Properties of Heavy Oil/Water ($NaHCO_3$) without Polymer. *Dynamic Interfacial Tensions.* Figure 3 shows the dynamic interfacial tension plotted as a function of time for increased concentrations of heavy oil in toluene. The dynamic interfacial tension for the oil/buffer interface at each concentration of heavy oil in toluene decreased slightly during the aging time. The data were fitted using eq 1 with high correlation coefficients R^2 ranging from 0.94 to 0.98.

Table 2 shows the data for the equilibrium interfacial tension σ^{eq} calculated from the fitted lines in Figure 3 for various concentrations of heavy oil in toluene. The CAC corresponded to 0.219 mol·kg^{-1} heavy oil in toluene. The fit of the data to eq 2 gave an average Gibbs surface excess of $9.17 \cdot 10^{-7}$ mol·m^{-2} and an area coverage per molecule of 1.81 nm^2. These values are consistent with previous data for higher °API heavy oils and asphaltenes.[5,6,48]

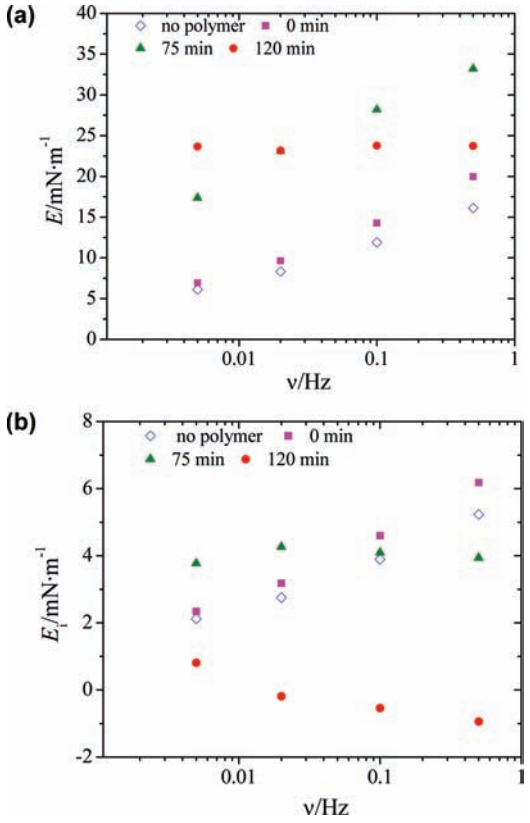

Figure 9. (a) E and (b) E_i as functions of frequency (ν) for a 0.183 mol·kg^{-1} heavy-oil-in-toluene−$NaHCO_3$ interface containing $2.5 \cdot 10^{-9}$ mol·kg^{-1} polymer at (0, 75, and 120) min. Data for an interface containing no polymer in the water phase are shown for comparison.

Interfacial Rheology of the Control. The interfacial rheology of the control was performed using drops of 0.183 mol·kg^{-1} heavy oil in toluene immersed in 0.01 mol·kg^{-1} $NaHCO_3$. This ensured that the interfacial conditions were slightly below the CAC of 0.219 mol·kg^{-1} heavy oil. Controlled dilational oscillation started after aging of the drop for 15 h. Figure 4 shows parallel and similar increases in the viscoelastic modulus E with the elastic modulus E_0 (the elastic component) as the frequency increased for the stable 0.183 mol·kg^{-1} heavy-oil-in-toluene droplet. The interface showed a lower viscous modulus component that was also frequency-dependent. The viscous modulus E_i was less than elastic modulus E_0 at all frequencies, thus confirming a dominant elastic property of the oil droplet interface. Although the viscous modulus E_i increased with increasing oscillation frequency, it did not show as steep a gradient. The phase angle ϕ decreased slightly, while there was a rise in viscoelasticity with oscillation frequency. This suggests a rearrangement of the natural adsorbed interfacial material that effected an enhancement in the interfacial viscoelasticity.

Interfacial Properties of Heavy Oil/Water ($NaHCO_3$) after Polymer Addition. *Dynamic Interfacial Tensions.* A polymer solution with a concentration as high as $5 \cdot 10^{-6}$ mol·kg^{-1}in 0.01 mol·kg^{-1} $NaHCO_3$ caused a reduction in the surface tension of the $NaHCO_3$ solution from (73.9 to 52.2) mN·m^{-1}. Low polymer concentrations [(0 to 25)·10^{-9} mol·kg^{-1}] did not significantly affect the interfacial tension of the toluene−water interface. This indicated its purity. Its negligible interfacial activity confirmed that the polymer was not very surface active by itself. However, when the polymer interacted with the heavy oil−water interface, it enhanced its interfacial activity considerably. Figure 5 shows the dynamic interfacial tension σ_{dyn} for the oil−water interface measured at increasing concentrations of polymer added to the water phase in comparison with the control without polymer.

There was an initial decline in σ_{dyn} followed by a flattening of the σ_{dyn}-versus-time curves for systems with less than $6.25 \cdot 10^{-9}$ mol·kg^{-1} polymer. A second sharper gradient of σ_{dyn} with time followed. The second $\Delta\sigma_{dyn}/\Delta t$ gradient was smaller for lower concentrations of polymer [(2.5 and 6.25)·10^{-9} mol·kg^{-1}]. This indicated rearrangements of adsorbed material at the interface, thus promoting a faster decline in interfacial tension with time. For the highest concentration of added polymer ($25 \cdot 10^{-9}$ mol·kg^{-1}), the σ_{dyn}-versus-time curve showed an immediate decline and a sharp $\Delta\sigma_{dyn}/\Delta t$ gradient. This behavior suggests that charge neutralization of droplets observed earlier by the attraction of the positively charged polymer to the negatively charged groups of the heavy oil caused the interface material to be reorganized, thereby enhancing the interfacial activity synergistically. The sharp gradients indicate that Marangoni flows occurred at the interface to enhance the interfacial activity. However, the interfacial rheological data shown next provide more insight into these effects.

Interfacial Rheology after Polymer Addition. Figure 6a−d shows the effects of polymer adsorption dynamics at various frequencies of drop oscillation by comparing plots of E, E_0, E_i, and ϕ, respectively, as functions of polymer concentration. The curves for the complex viscoelastic modulus E and elastic modulus E_0 are similar, showing a steady rise with increasing oscillation frequency at each polymer concentration. However, the behaviors of the drops for polymer concentrations below $0.5 \cdot 10^{-9}$ mol·kg^{-1} appeared to be the same at all frequencies. There was a slight rise in E and E_0 from (0.5 to 2.5)·10^{-9} mol·kg^{-1}, after which these values increased sharply. This indicates that reorientation of the polymer occurred, resulting in enhanced viscoelasticity during relaxation. Below $0.25 \cdot 10^{-9}$ mol·kg^{-1} polymer at all frequencies, the viscous modulus E_i in Figure 6c remained steadily constant. The E_i values were lower than the values of the elastic modulus E_0 (Figure 6b) at all frequencies and polymer dosages. A steady rise in E_i with increasing frequency occurred for each dosage, indicating that the deformation rate increased and some flow occurred at the interface. Above $0.5 \cdot 10^{-9}$ mol·kg^{-1} polymer, E_i increased linearly to a maximum and then declined. Consistent with the E_0 responses to polymer dosage, the phase angle ϕ (Figure 6d) remained virtually unchanged for polymer concentrations below $2.5 \cdot 10^{-9}$ mol·kg^{-1}, and the values were highest at the lowest frequency of 0.005 Hz and lowest at 0.5 Hz. This indicates a rise in the viscoelastic property of the interface with increasing frequency as well as above $2.5 \cdot 10^{-9}$ mol·kg^{-1} polymer.

The indications of changes in dilational viscosity arising from internal reorientation of the adsorbed layers of the heavy oil drop led us to examine plots of the moduli as functions of frequency. Figure 7a−c shows the frequency responses for polymer dosages of ($1 \cdot 10^{-11}$, $2.5 \cdot 10^{-9}$, and $12.5 \cdot 10^{-9}$) mol·kg^{-1} relative to the control in Figure 4. All of the systems were dominated by the elastic modulus E_0, which paralleled the rising viscoelastic modulus E as the frequency increased. The frequency-dependent characteristic behaviors of E and E_0 were dominant for these polymer dosages and enhanced at the higher dosages. The E_i was only slightly dependent on the oscillation frequency for the $12.5 \cdot 10^{-9}$ mol·kg^{-1} system.

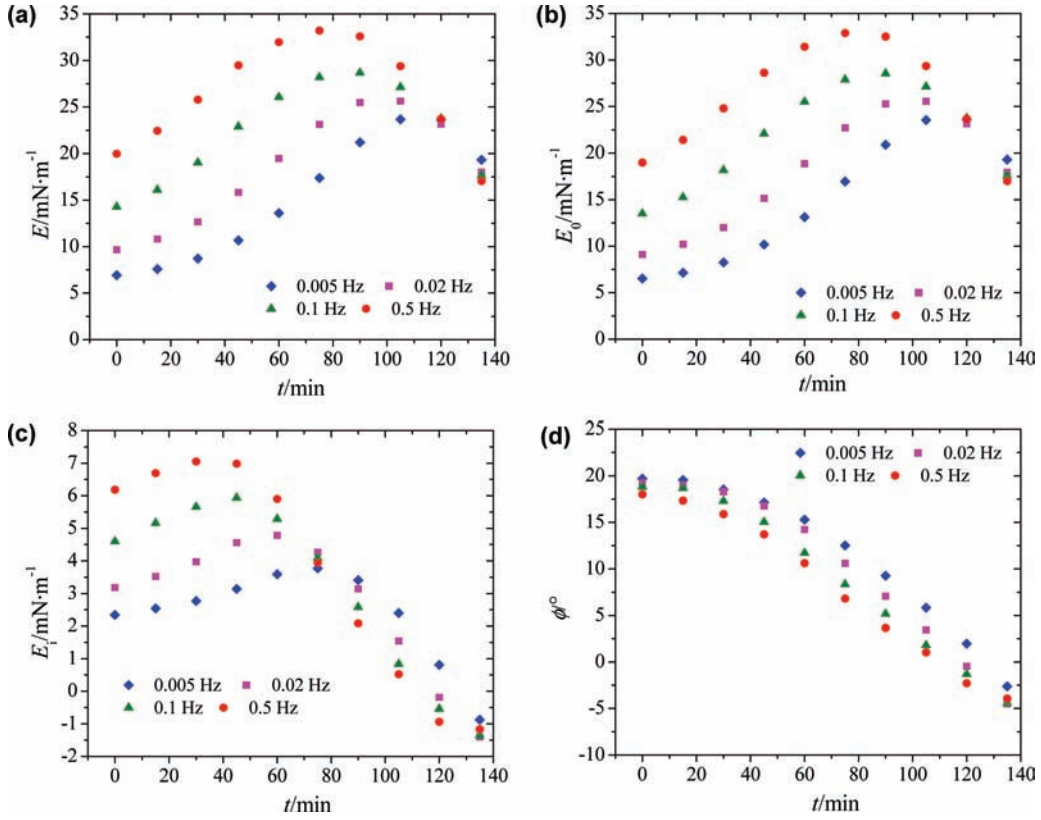

Figure 10. Plots of (a) E, (b) E_0, (c) E_i, and (d) ϕ as functions of residence time (t) for a 0.183 mol·kg^{-1} heavy-oil-in-toluene−$NaHCO_3$ interface with $2.5 \cdot 10^{-9}$ mol·kg^{-1} polymer in the water phase at (0.005, 0.02, 0.1, and 0.5) Hz.

Figure 8a,b shows the viscoelastic and viscous moduli, respectively, as functions of frequency, comparing the interfaces for all three dosages of polymer added and the control without polymer (0 mol·kg^{-1}). At $12.5 \cdot 10^{-9}$ mol·kg^{-1} polymer, E had the highest values at all frequencies, but E_i shifted to lower values above 0.1 Hz, indicating a decrease in the rate of interfacial deformation.

The behaviors of these systems suggest that time is important for the adsorption and the resulting viscoelastic properties. A comparison of the viscoelastic behaviors as a function of frequency for a $2.5 \cdot 10^{-9}$ mol·kg^{-1} polymer system at times 0, 75, and 120 min (Figure 9) shows that E and E_i change as time progresses. At 0 min, E for the $2.5 \cdot 10^{-9}$ mol·kg^{-1} system paralleled the control containing no polymer (0 mol·kg^{-1}) as the frequency increased. At 75 min, E increased to significantly higher values with frequency but remained unchanged at 120 min. At 75 min, E_i peaked at 0.02 Hz (Figure 9b) and then declined slightly to a constant value. At 120 min, E_i decreased with increasing frequency. Figure 10a−d shows plots of E, E_0, E_i, and ϕ, respectively, as functions of residence time for the same system at four frequencies. There was a logistic rise in E and E_0 to a maximum at a characteristic residence time, after which they declined to a constant lower value at 120 min, where increasing the frequency had no effect. The E maximum occurred at (75, 90, 105, and 105) min for (0.5, 0.1, 0.02, and 0.005) Hz respectively. The maximum E_i occurred after shorter times of (30, 45, 60, 75) min, respectively, for the same frequencies (Figure 10c). The phase angles ϕ decreased with time at all frequencies (Figure 10d). These behaviors are consistent with the occurrence of reorientation after the adsorption that causes charge neutralization, followed by charge reversal of the interface and perturbation of the interface.

CONCLUSIONS

In this work, we have shown the following:

1. In situ nanoemulsions of heavy oil in water were highly stable because of the high negative ζ potentials and nanosizes.
2. Nanoemulsions were destabilized by charge neutralization using a cationic polymer, but water-phase separation was a kinetically controlled process, as evidenced by drop-size growth, microscopy, and water resolution in time.
3. The dynamic interfacial tension data for the heavy oil−water interface at various oil concentrations were used to determine the monolayer coverage at 0.219 mol·kg^{-1} heavy oil in toluene. The Gibbs surface excess was found to be $9.17 \cdot 10^{-7}$ mol·m^{-2} and the area per mole of oil was 1.81 nm^2·mol^{-1}, consistent with previous findings.
4. The addition of the cationic polymer to a stable 0.183 mol·kg^{-1} oil−water interface caused enhanced interfacial activity with a faster decline in dynamic interfacial tension in time as the polymer concentration in water increased.
5. Without polymer, the interfacial rheological data for the oil−water interface showed that the interfacial viscoelasticity increased with drop oscillation frequency.
6. There were large increases in the interfacial viscoelastic moduli with increasing frequency and as polymer concentration in the water phase increased, causing charge neutralization.
7. These viscoelastic properties were time- and frequency-dependent for lower polymer dosages and became less

dx.doi.org/10.1021/je101162n |J. Chem. Eng. Data 2011, 56, 1388–1396

frequency dependent at longer times at higher polymer dosages. The E_i showed a peak at $12.5 \cdot 10^{-9}$ mol·kg^{-1}.

8. Characteristic time maxima for E, E_0, and E_i were observed for the critical dosage of polymer added at each frequency.

AUTHOR INFORMATION

Corresponding Author

*E-mail: angle@nrcan.gc.ca.

Funding Sources

Funding for this work was obtained from the Government of Canada, NRCan, CanmetENERGY, in Devon.

ACKNOWLEDGMENT

Rachel Ghent conducted some of the experiments for part of the data.

REFERENCES

(1) Angle, C. W. Effects of sand fraction on toluene−diluted heavy oil in water emulsions in turbulent flow. *Can. J. Chem. Eng.* **2004**, *82*, 722–734.

(2) Angle, C. W.; Lue, L.; Dabros, T.; Hamza, H. A. Viscosities of heavy oils-in-toluene and partially deasphalted heavy oils-in-Heptol in a study of asphaltenes self-interactions. *Energy Fuels* **2005**, *19*, 2014–2020.

(3) Angle, C. W.; Long, Y.; Hamza, H. A.; Lue, L. Precipitation of asphaltenes from solvent-diluted heavy oil and thermodynamic properties of solvent-diluted heavy oil solutions. *Fuel* **2006**, *85*, 492–506.

(4) Angle, C. W.; Hamza, H. A. Drop sizes during turbulent mixing of toluene−heavy oil fractions in water. *AIChE J.* **2006**, *52*, 2639–2650.

(5) Angle, C. W.; Hamza, H. A.; Dabros, T. Size distributions and stability of toluene-diluted heavy oil emulsions. *AIChE J.* **2006**, *52*, 1257–1266.

(6) Angle, C. W.; Dabros, T.; Hamza, H. A. Predicting the sizes of toluene-diluted heavy oil emulsions in turbulent flow. Part 1. Application of two adsorption kinetic models for σ^E in two size predictive models. *Chem. Eng. Sci.* **2006**, *61*, 7309–7324.

(7) Angle, C. W.; Hamza, H. A. Predicting the sizes of toluene-diluted heavy oil emulsions in turbulent flow. Part 2. Hinze−Kolmogorov based model adapted for increased oil fractions and energy dissipation in a stirred tank. *Chem. Eng. Sci.* **2006**, *61*, 7325–7335.

(8) Angle, C. Stability of heavy oil emulsions in turbulent flow and different chemical environments. Ph.D. thesis, University of Manchester Institute of Science and Technology, Manchester, U.K., 2004.

(9) Dicharry, C.; Arla, D.; Sinquin, A.; Graciaa, A.; Bouriat, P. Stability of water/crude oil emulsions based on interfacial dilatational rheology. *J. Colloid Interface Sci.* **2006**, *297*, 785–791.

(10) Hannisdal, A.; Hemmingsen, P. V.; Silset, A.; Sjoblom, J. Stability of Water/Crude Oil Systems Correlated to the Physicochemical Properties of the Oil Phase. *J. Dispersion Sci. Technol.* **2007**, *28*, 639–652.

(11) Hannisdal, A.; Orr, R.; Sjoblom, J. Viscoelastic properties of crude oil components at oil−water interfaces. 1. The effect of dilution. *J. Dispersion Sci. Technol.* **2007**, *28*, 81–93.

(12) Hannisdal, A.; Orr, R.; Sjoblom, J. Viscoelastic properties of crude oil components at oil−water interfaces. 2: Comparison of 30 oils. *J. Dispersion Sci. Technol.* **2007**, *28*, 361–369.

(13) Menon, V. B.; Wasan, D. T. Particle Fluid Interactions with Application to Solid-Stabilized Emulsions 0.1. the Effect of Asphaltene Adsorption. *Colloids Surf.* **1986**, *19*, 89–105.

(14) Poteau, S.; Argillier, J. F.; Langevin, D.; Pincet, F.; Perez, E. Influence of pH on stability and dynamic properties of asphaltenes and other amphiphilic molecules at the oil−water interface. *Energy Fuels* **2005**, *19*, 1337–1341.

(15) Quintero, C. G.; Noik, C.; Dalmazzone, C.; Grossiord, J. L. Formation Kinetics and Viscoelastic Properties of Water/Crude Oil Interfacial Films. *Oil Gas Sci. Technol.* **2009**, *64*, 607–616.

(16) Yarranton, H. W.; Sztukowski, D. M.; Urrutia, P. Effect of interfacial rheology on model emulsion coalescence. I. Interfacial rheology. *J. Colloid Interface Sci.* **2007**, *310*, 246–252.

(17) Angle, C. W. *Encylopedic Handbook of Emulsion Technology*; Marcel Dekker: New York, 2001; Chapter 24, pp 541−594.

(18) Angle, C. W.; Dabros, T.; Hamza, H. A. Demulsifier effectiveness in treating heavy oil emulsions in the presence of fine sands in the production fluids. *Energy Fuels* **2007**, *21*, 912–919.

(19) Alvarez, G.; Poteau, S.; Argillier, J. F.; Langevin, D.; Salager, J. L. Heavy Oil−Water Interfacial Properties and Emulsion Stability: Influence of Dilution. *Energy Fuels* **2009**, *23*, 294–299.

(20) Aske, N.; Orr, R.; Sjoblom, J. Dilatational elasticity moduli of water−crude oil interfaces using the oscillating pendant drop. *J. Dispersion Sci. Technol.* **2002**, *23*, 809–825.

(21) Aske, N.; Orr, R.; Sjoblom, J.; Kallevik, H.; Oye, G. Interfacial properties of water−crude oil systems using the oscillating pendant drop. Correlations to asphaltene solubility by near infrared spectroscopy. *J. Dispersion Sci. Technol.* **2004**, *25*, 263–275.

(22) Bauget, F.; Langevin, D.; Lenormand, R. Dynamic surface properties of asphaltenes and resins at the oil−air interface. *J. Colloid Interface Sci.* **2001**, *239*, 501–508.

(23) Bouriat, P.; El Kerri, N.; Graciaa, A.; Lachaise, J. Properties of a two-dimensional asphaltene network at the water−cyclohexane interface deduced from dynamic tensiometry. *Langmuir* **2004**, *20*, 7459–7464.

(24) Czarnecki, J.; Moran, K. On the stabilization mechanism of water-in-oil emulsions in petroleum systems. *Energy Fuels* **2005**, *19*, 2074–2079.

(25) Daniel-David, D.; Pezron, I.; Dalmazzone, C.; Noik, C.; Clausse, D.; Komunjer, L. Elastic properties of crude oil/water interface in presence of polymeric emulsion breakers. *Colloids Surf., A* **2005**, *270*, 257–262.

(26) Freer, E. M.; Radke, C. J. Relaxation of asphaltenes at the toluene/water interface: Diffusion exchange and surface rearrangement. *J. Adhes.* **2004**, *80*, 481–496.

(27) Moran, K. Dilational elasticity of emulsified bitumen droplet surfaces. *J. Dispersion Sci. Technol.* **2007**, *28*, 399–406.

(28) Moran, K.; Sumner, R. J. Aging effects on surface properties and coalescence of bitumen droplets. *Can. J. Chem. Eng.* **2007**, *85*, 643–653.

(29) Sztukowski, D. M.; Yarranton, H. W. Oilfield solids and water-in-oil emulsion stability. *J. Colloid Interface Sci.* **2005**, *285*, 821–833.

(30) Spiecker, P. M.; Kilpatrick, P. K. Interfacial rheology of petroleum asphaltenes at the oil−water interface. *Langmuir* **2004**, *20*, 4022–4032.

(31) Sun, T. L.; Zhang, L.; Wang, Y. Y.; Zhao, S.; Peng, B.; Li, M. Y.; Yu, J. Y. Influence of demulsifiers of different structures on interfacial dilational properties of an oil−water interface containing surface-active fractions from crude oil. *J. Colloid Interface Sci.* **2002**, *255*, 241–247.

(32) Sun, T. L.; Zhang, L.; Wang, Y. Y.; Peng, B.; Zhao, S.; Li, M. Y.; Yu, J. Y. Dynamic dilational properties of oil−water interfacial films containing surface active fractions from crude oil. *J. Dispersion Sci. Technol.* **2003**, *24*, 699–707.

(33) Sztukowski, D. M.; Yarranton, H. W. Rheology of asphaltene—Toluene/water interfaces. *Langmuir* **2005**, *21*, 11651–11658.

(34) Wang, Y. Y.; Zhang, L.; Sun, T. L.; Zhao, S.; Yu, J. Y. A study of interfacial dilational properties of two different structure demulsifiers at oil−water interfaces. *J. Colloid Interface Sci.* **2004**, *270*, 163–170.

(35) Wang, Z. B.; Narsimhan, G. Interfacial dilatational elasticity and viscosity of β-lactoglobulin at air−water interface using pulsating bubble tensiometry. *Langmuir* **2005**, *21*, 4482–4489.

(36) Yang, X. L.; Verruto, V. J.; Kilpatrick, P. K. Dynamic asphaltene−resin exchange at the oil/water interface: Time-dependent W/O emulsion stability for asphaltene/resin model oils. *Energy Fuels* **2007**, *21*, 1343–1349.

(37) Yarranton, H. W.; Urrutia, P.; Sztukowski, D. M. Effect of interfacial rheology on model emulsion coalescence. II. Emulsion coalescence. *J. Colloid Interface Sci.* **2007**, *310*, 253–259.

(38) Cao, X. L.; Li, Y.; Jiang, S. X.; Sun, H. Q.; Cagna, A.; Dou, L. X. A study of dilational rheological properties of polymers at interfaces. *J. Colloid Interface Sci.* **2004**, *270*, 295–298.

(39) Chaverot, P.; Cagna, A.; Glita, S.; Rondelez, F. Interfacial tension of bitumen−water interfaces. Part 1: Influence of endogenous surfactants at acidic pH. *Energy Fuels* **2008**, *22*, 790–798.

(40) Verruto, V. J.; Le, R. K.; Kilpatrick, P. K. Adsorption and Molecular Rearrangement of Amphoteric Species at Oil−Water Interfaces. *J. Phys. Chem. B* **2009**, *113*, 13788–13799.

(41) Leser, M. E.; Acquistapace, S.; Cagna, A.; Makievski, A. V.; Miller, R. Limits of oscillation frequencies in drop and bubble shape tensiometry. *Colloids Surf., A* **2005**, *261*, 25–28.

(42) Miller, R.; Liggieri, L. Interfacial rheology—The response of two-dimensional layers on external perturbations. *Curr. Opin. Colloid Interface Sci.* **2010**, *15*, 215–216.

(43) Ravera, F.; Loglio, G.; Pandolfini, P.; Santini, E.; Liggieri, L. Determination of the dilational viscoelasticity by the oscillating drop/bubble method in a capillary pressure tensiometer. *Colloids Surf., A* **2010**, *365*, 2–13.

(44) Ravera, F.; Ferrari, M.; Santini, E.; Liggieri, L. Influence of surface processes on the dilational visco-elasticity of surfactant solutions. *Adv. Colloid Interface Sci.* **2005**, *117*, 75–100.

(45) Ravera, F.; Loglio, G.; Kovalchuk, V. I. Interfacial dilational rheology by oscillating bubble/drop methods. *Curr. Opin. Colloid Interface Sci.* **2010**, *15*, 217–228.

(46) Cui, X. H.; Zhang, L.; Luo, L.; Zhang, L.; Zhao, S.; Yu, J. Y. Interfacial dilational properties of model oil and chemical flooding systems by relaxation measurements. *Colloids Surf., A* **2010**, *369*, 106–112.

(47) Benjamins, J.; Cagna, A.; Lucassen-Reynders, E. H. Viscoelastic properties of triacylglycerol/water interfaces covered by proteins. *Colloids Surf., A* **1996**, *114*, 245–254.

(48) Lucassen-Reynders, E. H.; Cagna, A.; Lucassen, J. Gibbs elasticity, surface dilational modulus and diffusional relaxation in nonionic surfactant monolayers. *Colloids Surf., A* **2001**, *186*, 63–72.